Abdominal Radiology

Published online: 1 April 2017

Abdom Radiol (2017) 42:2261–2271
DOI: 10.1007/s00261-017-1119-2

Magnetic resonance findings of hepatic epithelioid hemangioendothelioma: emphasis on hepatobiliary phase using Gd-EOB-DTPA

Jeong Hyun Lee,[1] Woo Kyoung Jeong,[1] Young Kon Kim,[1] Won Jae Lee,[1] Sang Yun Ha,[2] Kyoung Won Kim,[3] Jihun Kim[4]

[1]Department of Radiology and Center for Imaging Sciences, Samsung Medical Center, Sungkyunkwan University School of Medicine, 81 Irwon-ro, Gangnam-gu, Seoul 06351, Korea
[2]Department of Pathology, Samsung Medical Center, Sungkyunkwan University School of Medicine, Seoul, Korea
[3]Department of Radiology, Asan Medical Center, University of Ulsan College of Medicine, Seoul, Korea
[4]Department of Pathology, Asan Medical Center, University of Ulsan College of Medicine, Seoul, Korea

Abstract

Purpose: To examine the characteristic features of hepatic epithelioid hemangioendothelioma (HEH) on magnetic resonance imaging (MRI) using Gd-EOB-DTPA.

Material and methods: Twelve patients (mean age, 50 years; male:female = 6:6) who were pathologically confirmed to have HEH in two tertiary institutions were retrospectively investigated. For qualitative analysis, the MRI features of HEH including core pattern were characterized, and lesions were divided into core and non-core groups. For quantitative analysis, standardized mean signal intensities (SI_{st}) measured at the tumor center, periphery, and liver parenchyma were plotted against the dynamic phases. Differences in SI_{st} between the core and non-core group were calculated for the tumor center and periphery. We also examined the radiologic and pathologic correlation for cases in which surgical resection was performed.

Results: Forty-seven nodules in 12 patients were analyzed. The mean size of the lesions was 2.9 ± 1.0 cm. In the per-lesion analysis, ring-like arterial enhancement (74%) on arterial phase was the most frequent feature, followed by core pattern (51%), and hyperintense rim on T1-weighted imaging (43%). In the per-patient analysis, capsular retraction (75%) was the most common sign. The percentage of patients with core pattern was 58%. In the core group, the SI_{st} of the center showed slow enhancement starting from the transitional phase, resulting in divergence between the two graphs throughout the entire dynamic study ($p < 0.05$). Pathologically, the lesion center consisted of reduced cellularity with myxohyaline stroma and necrosis.

Conclusion: Core pattern can be considered a new diagnostic sign of HEH.

Key words: Hepatic epithelioid hemangioendothelioma—Hepatobiliary phase—MRI—Gd-EOB-DTPA

Hepatic epithelioid hemangioendothelioma (HEH) is a rare tumor of vascular origin with unknown etiology and low to intermediate malignancy potential [1–3]. In contrast to other vascular tumors such as angiosarcoma or hemangioma, HEHs consist of dendritic and epithelioid tumor cells infiltrating hepatic sinusoidal spaces [3, 4]. The age at diagnosis spans from the second to ninth decade, with a peak incidence in the third decade, and there is a small female predilection with a female-to-male ratio of approximately 1.5 to 1 [1, 5]. The clinical presentation is usually non-specific and highly variable, ranging from asymptomatic cases to presentation with portal hypertension or hepatic failure [1, 6]. Prognosis of this disease is relatively good compared with other hepatic malignancies, especially the primary vascular malignancy angiosarcoma; however, outcome of the disease is also diverse, showing a correlation with pathologic features such as high cellularity [5]. Patients who do not receive any kind of treatment have a 5-year survival rate of approximately 40–50% [1, 5, 6]. Estab-

Correspondence to: Woo Kyoung Jeong; *email:* jeongwk@gmail.com

Table 1. MR imaging protocols

Sequence	TR/TE	FA	Matrix size	Section thickness (mm)	Intersection gap (mm)	No. of signals
Hospital A						
T1W-dual GRE	3.5/1.2–2.3	10	256 × 194	6	6	1
MS-T2WI*	1476.5/70	90	256 × 260	5	5	1
SS-T2WI*	1131.3/80	90	376 × 273	5	5	2
HT2WI*	1328.5/160	90	376 × 273	5	5	2
DWI*	1444/55	90	112 × 108	5	6	2
T1 W-3D GRE*	3.1/1.5	10	252 × 251	4.4	2.2	1
Hospital B						
T1W-dual GRE	164/2.3–4.6	70	256 × 192	6	1.2	1
HT2WI*	1100/151	150	256 × 192	6	1.2	1
T2WI*	4023–5755/85	150	384 × 288	6	1.2	2
DWI*	4800/73	180	150 × 128	6	1.2	5
CE Dyn.T1*	4.1/1.5	10	320 × 260	3	0	1

FA flip angle, *GRE* gradient echo, *MS-T2WI* multishot T2-weighted image, *SS-T2WI* single-shot T2-weighted image, *HT2WI* heavily T2-weighted image, *T2WI* T2-weighted image, CE Dyn. *T1* Contrast-enhanced dynamic T1-weighted image, * Fat saturation images

lishing the diagnosis can be difficult even with pathologic evaluation, especially when the specimen is sampled by fine-needle aspiration or needle core biopsy [7, 8]. It is therefore important for radiologists to raise suspicions when features of HEH are encountered [1, 7].

Although there are several publications in the literature describing the typical imaging features of HEH [3, 4, 7, 9, 10], it is still a challenge to recognize this entity in clinical practice because it resembles metastatic liver tumors rather than vascular tumors on imaging studies. Recently, the contrast agent Gd-EOB-DTPA has gained popularity due to its ease of use and characteristic distribution in the hepatobiliary system; specifically, it is taken up by normal hepatocytes and subsequently excreted into the biliary system. The hepatobiliary phase, about 20 min after Gd-EOB-DTPA administration, does not only help to detect focal hepatic lesions, but also help to characterize the lesions with specific features such as focal nodular hyperplasia [11, 12]. To date, there is no study focusing on the imaging features of HEH using Gd-EOB-DTPA. The purpose of this study was to evaluate several documented MRI signs of HEH and to analyze features on the hepatobiliary phase (HBP) using Gd-EOB-DTPA, with the aim of discovering a diagnostic sign of HEH.

Materials and methods

Patients

This retrospective study was approved by the institutional review boards of two university hospitals (IRB No.: SMC-2016-7-100, AMC-2016-0829), and the need for informed consent from the patients was waived. We collected cases for this study from the database of patients admitted at two hospitals. From February 2010 to March 2014, six patients at Samsung Medical Center (Hospital A) were pathologically proven to have HEH after undergoing contrast-enhanced MR imaging using Gd-EOB-DTPA. Also, from September 2009 to October 2013, another six patients were diagnosed with HEH after Gd-EOB-DTPA enhanced MR imaging at Asan Medical Center (Hospital B). The study population consisted of six males and six females with a mean age at diagnosis of 50 years (range 35–81 years). Seven patients were confirmed to have HEH after undergoing partial or total hepatectomy.

Image acquisition

MRI examinations were performed on a 1.5-T scanner or a 3.0-T scanner with a 16- or 32-channel phased-array coil as the receiver. Routine MRI protocol included an axial T1-weighted in-phase and out-of-phase sequence, an axial breath-hold multishot T2-weighted sequence, and an axial respiratory-triggered single-shot T2-weighted and heavily T2-weighted sequence. For the contrast enhancement protocol, the two hospitals adopted different methods: conventional injection with fixed timing of vascular phases in Samsung Medical Center and test-bolus technique in Asan Medical Center. At Samsung Medical Center, 0.1 mL/kg of Gd-EOB-DTPA (Primovist, Bayer HealthCare, Berlin, Germany) was automatically administered intravenously via a power injector at a rate of 2 mL/s, followed by a 20-mL saline flush. Images were acquired in the precontrast phase (before contrast injection), arterial phase (20–35 s), portal venous phase (60 s), transitional phase (3 min), 10-min delayed phase, and 20-min delayed phase (the so-called HBP), using a T1-weighted 3-dimensional turbo field-echo sequence. Asan Medical Center used a test-bolus technique (scanning of the abdominal aortic aorta after injection of 1 mL of Gd-EOB-DTPA with a saline flush) followed by intravenous injection of 0.1 mL/kg of Gd-EOB-DTPA at 1 ml/s and a 20-mL saline flush. Arterial, portal, transitional, and HBP images were acquired at 5 s, 60–70 s, 3 min, and 20 min after peak, respectively. Detailed MRI acquisition parameters are shown in Table 1.

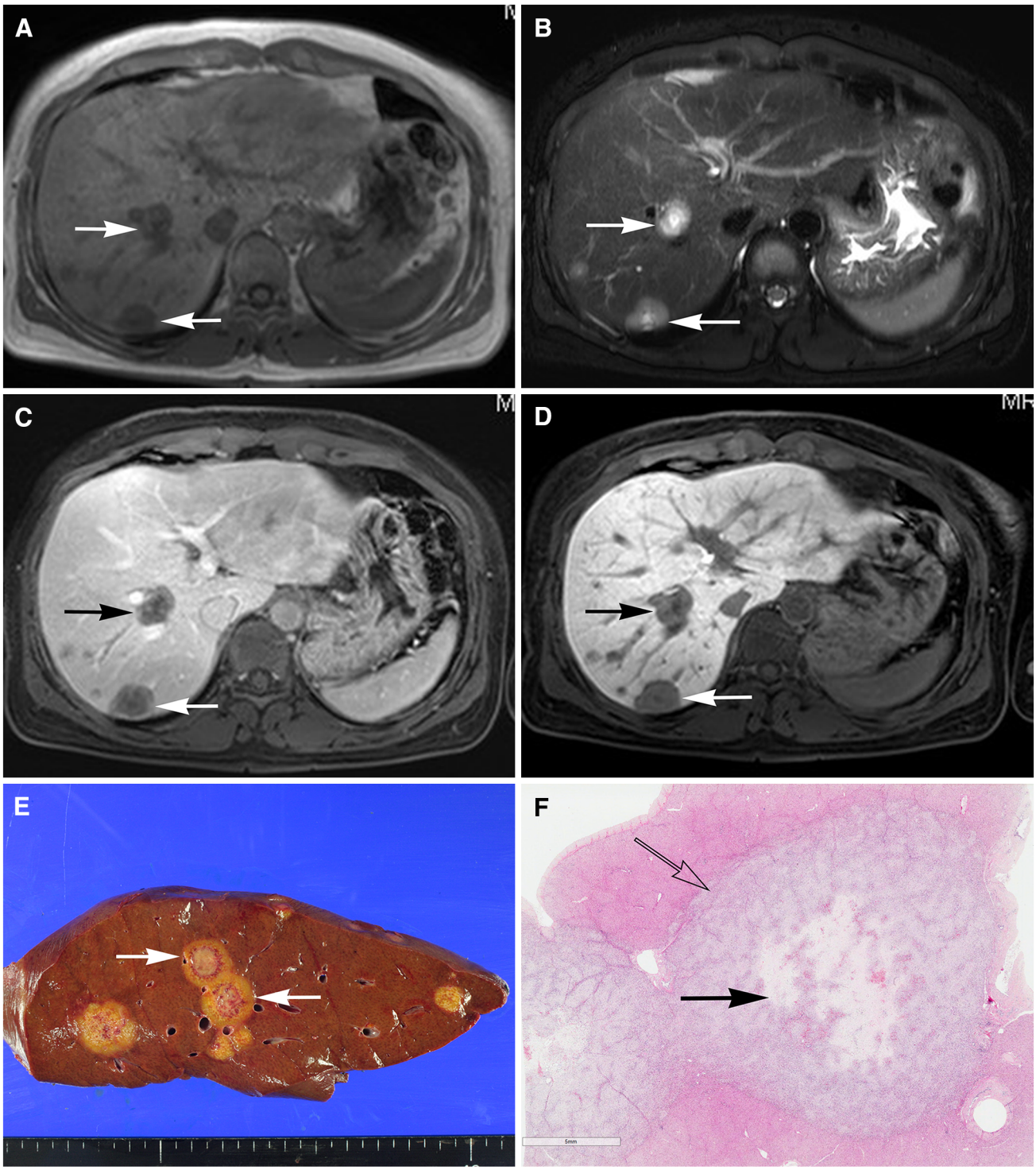

Fig. 1. Core pattern of hepatic epithelioid hemangioendothelioma (HEH). A 44-year-old female diagnosed with multiple HEH following explantation of the liver. T1- and T2-weighted images, respectively, show multiple round hypo- and hyperintense masses (*arrows*) that are coalescent (**A**, **B**). Portal venous phase image after administration of Gd-EOB-DTPA **C** shows that the signal intensity of the central portion (*arrows*) of the tumor is lower than that of periphery. The hepatobiliary phase **D** shows a target-like appearance of the tumor, termed the core pattern of HEH (*arrows*). On the gross specimen (**E**), a yellowish, infiltrating tumor is seen (*arrows*), corresponding to the coalescent tumors on MRI, and a mixed necrotic portion (*arrows*) with viable tumor cells (*open arrows*) is observed microscopically (H&E, X10; **F**).

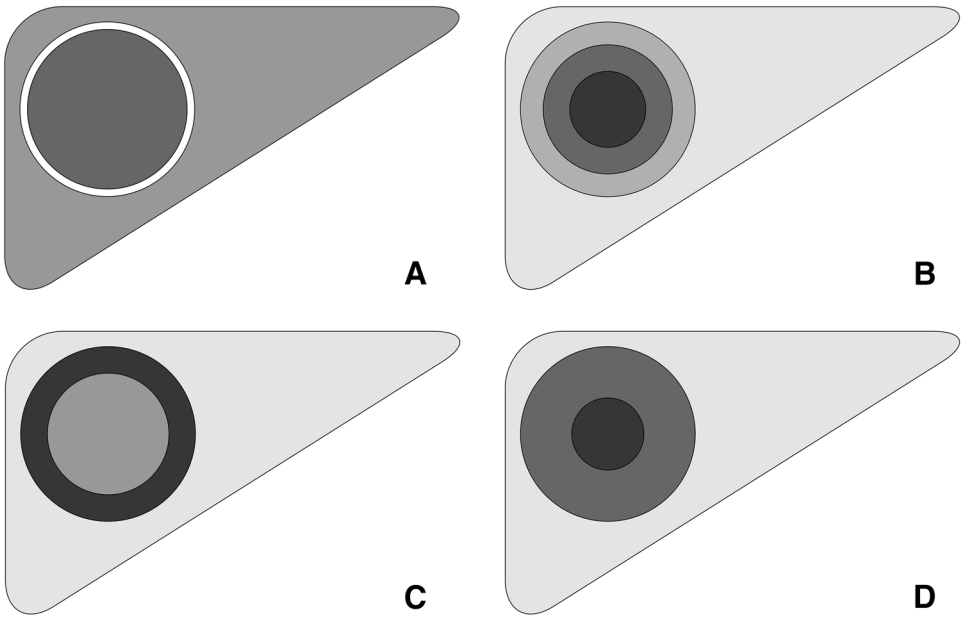

Fig. 2. Schematic of enhancement features. The ring-like arterial enhancement (**A**), layered enhancement pattern (**B**), entrapment-like pattern (**C**), and core pattern on the hepatobiliary phase (**D**).

Table 2. MR features of hepatic epithelioid hemangioendotheliomas and their incidences

Findings	Per lesion (n = 47)	Per patient (n = 12)		
		Dominant (present)	Mixed	Minor (absent)
Hypointense rim on T2WI	16 (34%)	2 (17%)	3 (25%)	7 (58%)
Hyperintense rim on T1WI	20 (43%)	4 (33%)	2 (17%)	6 (50%)
Ring-like arterial enhancement	35 (74%)	7 (58%)	3 (25%)	2 (17%)
Layered enhancement	19 (40%)	3 (25%)	4 (33%)	5 (42%)
Entrapment-like pattern	14 (30%)	2 (17%)	2 (17%)	8 (66%)
Core pattern	24 (51%)	4 (33%)	3 (25%)	5 (42%)
Coalescent morphology	N/A	7 (58%)	0	5 (42%)
Capsular retraction	N/A	9 (75%)	0	3 (25%)

T2WI T2-weighted image, *T1WI* T1-weighted image

MRI analysis and pathologic correlation

Two radiologists (W.K.J., with 10 years of experience in abdominal radiology, and J.H.L., with 3 years in radiology residency) reviewed all images in consensus for qualitative and quantitative analyses of MRI features of HEH. For convenience of analysis, in patients with multiple lesions, the five largest lesions were selected for analysis. For qualitative analysis, we evaluated several morphologic characteristics that had been described in previous reports [13, 14]. On per-lesion analysis, the incidence of hypointense rim on T2-weighted images, hyperintense rim on T1-weighted images, ring-like arterial enhancement, layered enhancement, entrapment-like pattern, or core pattern was calculated from the pooled lesions of all patients. Size was measured at the longest diameter on axial images. Hypo- and hyperintensity of the rim was determined by comparing the signal intensity to the center of the mass on T2- and T1-weighted image, respectively. Ring-like arterial enhancement was defined as a thin peripheral enhancement encircling the lesion on arterial phase. Layered enhancement was present when the lesion appeared to show more than two layers with varying degrees of enhancement in a concentric configuration on either the portal or transitional phase. Entrapment-like pattern was present when the lesion center showed higher signal intensity than the lesion periphery on HBP [13]. Core pattern, which we suspected as a novel imaging feature of HEH, was present when a seed-like and distinct center of low signal intensity could be identified on HBP (Fig. 1A, B). A schematic of the enhancement features is presented in Fig. 2.

On per-patient analysis, each of the above features and the presence of coalescent morphology and capsular retraction were evaluated. Coalescing pattern was present when the lesion seemed to be formed by overlapping lesions. Capsular retraction was present when the adjacent liver surface was retracted toward the lesion. Core pattern, hypointense rim on T2-weighted images, hyperintense rim on T1-weighted images, ring-like arterial enhancement, layered enhancement, and entrapment-like pattern were defined as ‘‘dominant’’ when

more than 75% of the designated lesions in the same patient exhibited the feature; "minor" when fewer than 25% of the lesions did; and "mixed" when the incidence was >25% but <75%.

For quantitative analysis of core pattern in the mass on dynamic contrast-enhanced study, average signal intensity calculated from manually drawn oval regions of interest (ROI) measuring approximately 10 mm^2 were acquired from the following four locations on the same axial image: the center of the lesion (SI_c), periphery of the lesion (SI_{pp}), hepatic parenchyma (SI_{par}), and paraspinal muscles (SI_{mus}). Care was taken not to include inhomogeneous regions, such as regions with traversing vessels and artifacts. All values were the average of three separate, non-overlapping measurements. For standardization, values of the lesion center, lesion periphery, and hepatic parenchyma were divided by the average signal intensity of the paraspinal muscles on the same axial image (Standardized signal intensity (SI_{st}) = $SI_{c\ or\ pp\ or\ par}/SI_{mus}$). The standardized signal intensity (SI_{st}) was then averaged per vascular phase and plotted against each phase of the dynamic study. Separate plots for core and non-core lesions were drawn. Additionally, SI_{st} of the lesion center and periphery was compared between the two groups for each phase.

We also examined the surgical specimens of seven patients for radiologic–pathologic correlation. Two liver pathologists (S.Y.H. in Samsung Medical Center; J.K. in Asan Medical Center) reviewed the resected liver for histopathologic features of HEHs. All specimens were examined by hematoxylin and eosin staining and immunohistochemical analyses to confirm the diagnosis.

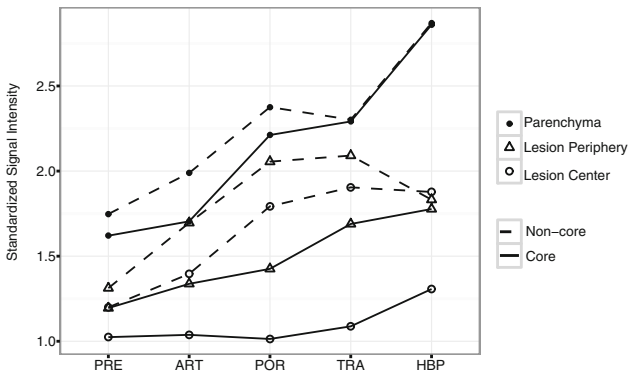

Fig. 3. Comparison of standardized signal intensity on dynamic Gd-EOB-DTPA-enhanced MRI between core and non-core pattern groups of hepatic epithelioid hemangioendothelioma (HEH). In the core pattern group, the SI_{st} of the tumor center does not increase until the transitional phase, resulting in substantial difference of the SI_{st} between the periphery and center on HBP. In the non-core pattern group, the SI_{st} of center and periphery increase in parallel, and the signal intensities of the two portions are nearly the same on HBP. *PRE* precontrast phase, *ART* arterial phase, *POR* portal phase, *TRA* transitional phase, *HBP* hepatobiliary phase.

The pathologic diagnosis was based on microscopic findings of characteristic proliferation of dendritic or epithelioid cells with abundant eosinophilic cytoplasm and occasional intracytoplasmic vacuolization in myxoid or fibrous stroma, and positivity for vascular markers such as CD31, CD34 or Factor VIII-associated antigen on immunohistochemistry. For the radiologic–pathologic correlation, the pathologists reviewed the slides with the radiologists who had reviewed the MR features of HEH. Additionally, we observed the patients' outcome after treatment and investigated associations between MRI features and outcome.

Statistical analysis

We calculated the frequency of the qualitative imaging features on per-lesion and per-patient bases. χ^2 test was performed for analysis of relationships among non-parametric variables such as MR features. Next, we performed generalized estimating equation for comparison of the SI_{st} of the lesion center and periphery between lesions that showed a core pattern and those that did not because some quantitative data were measured repeatedly in the same patients. The SI_{st} was measured and compared on each of the dynamic phases. χ^2 tests were performed to investigate which imaging findings were more frequently observed in the patients who were alive without any problems, compared to those who either showed unfavorable outcome or were lost to follow-up. All statistical analyses were performed using SPSS Statistics software (version 23; IBM, Armonk, NY). A p value <0.05 was considered to indicate a statistically significant difference.

Results

MR features of HEH

A total of 47 lesions from 12 patients were included in the qualitative and quantitative analysis. The total number of lesions was ≥5 in eight patients (67%), 3 in one patient, 2 in one patient, and 1 in two patients. The mean size of the lesions was 2.9 cm, ranging from 1.0 cm to 8.7 cm (standard deviation, 1.8 cm). The incidence of each predetermined finding on per-lesion analysis is summarized in Table 2. The most common feature was ring-like enhancement on arterial phase (n = 35; 74%). Core pattern was also a common finding, found in 24 lesions (51%), followed by hyperintense rim on T1-weighted images (n = 20; 43%), layered enhancement pattern (n = 19, 40%), hypointense rim on T2-weighted images (n = 16, 34%), and entrapment-like pattern (n = 14, 30%). For quantitative analysis, the mean SI_{st} of the center of the lesions, periphery of the lesions, and hepatic parenchyma was plotted against the sequential dynamic phases for the core group and non-core group as presented in Fig. 3. Values of the plot are presented in Table 3. In the non-core group, the SI_{st} of the center

Table 3. Comparison of standardized signal intensity (SI_{st}) between core and non-core pattern lesions

Phases of enhancement	Lesion center			Lesion periphery		
	Non-core	Core	*p* value	Non-core	Core	*p* value
Pre	1.20 ± 0.06	1.02 ± 0.07	0.040	1.31 ± 0.07	1.20 ± 0.07	0.177
Arterial	1.40 ± 0.08	1.04 ± 0.09	0.002	1.70 ± 0.19	1.34 ± 0.14	0.117
Portal	1.79 ± 0.26	1.01 ± 0.07	0.003	2.06 ± 0.28	1.43 ± 0.09	0.034
Transitional	1.90 ± 0.23	1.09 ± 0.09	0.001	2.09 ± 0.22	1.69 ± 0.10	0.089
HBP	1.88 ± 0.15	1.31 ± 0.09	0.001	1.83 ± 0.11	1.78 ± 0.12	0.726

Generalized estimating equation (GEE) for statistical analysis
Numbers are estimated marginal means ± standard errors of the means
p value <0.05 considered significant

showed a relatively small difference compared with the periphery and appeared to 'wash-out' on HBP. In contrast, the SI_{st} of the lesion center in the core group showed slow enhancement starting from the transitional phase, resulting in divergence between the two graphs throughout the entire dynamic study ($p < 0.05$, Table 3). The SI_{st} of the tumor center in the non-core lesion group was significantly higher than that in the core group during precontrast phase to HBP ($p < 0.05$).

In per-patient analysis, the most common finding was capsular retraction (present, $n = 9$; 75%) followed by ring-like arterial enhancement and coalescent morphology (dominant or present, $n = 7$; 58% for both). Core pattern was also a frequent finding (dominant and mixed, $n = 7$; 58%). Entrapment-like pattern was dominant in two patients, and two other patients had mixed entrapment and non-entrapment-like lesions (Table 2).

Radiologic–pathologic correlation

We were able to perform radiologic–pathologic correlation for seven cases (four patients with the core pattern, three patients without the core pattern) who underwent hepatic resection or total hepatectomy followed by liver transplantation. On pathological examination, a zonal pattern of cellularity, much like the core pattern on MRI, was seen in three out of four patients who exhibited the core pattern: the periphery of the tumors was highly cellular with tumor cells replacing the hepatic cords while the center was much less cellular and showed hyalinization or necrosis (Fig. 1). One patient who had the core pattern showed high cellularity without central necrosis. Two cases that did not have the core pattern had fibrotic stroma at the center of the tumor that showed an entrapment-like pattern on MRI corresponding to abundant fibrotic tissue and desmoplasia instead of central necrosis or tumor cells. One patient without the core pattern showed relatively abundant fibrosis.

Clinical outcomes of HEH

Table 4 summarizes the clinical courses of the patients. Five patients underwent partial hepatectomy and two patients underwent total hepatectomy with liver transplantation. The two patients who underwent liver transplantation died because of progression of metastasis ($n = 1$) and post-operative complication (biliary obstruction and cast formation; $n = 1$). The remaining patients were alive without any problems such as tumor recurrence or other complications. One patient who did not undergo surgical resection had lung metastasis at the time of diagnosis and decided not to receive any treatment. A middle-aged man diagnosed with HEH decided not to treat the lesion, and is still alive without tumor progression at 51 months. The remaining three patients who had no treatment were lost to follow-up within 3 months after diagnosis.

Six patients who were alive without progression after partial hepatectomy ($n = 5$) or alive without any treatment ($n = 1$) were classified into the "alive without any problem" group. This group showed multiplicity (50%; $n = 3$), core pattern (33%; $n = 2$), coalescence (50%; $n = 3$), capsular retraction (67%; $n = 4$), and entrapment-like pattern (17%; $n = 1$) on MRI studies. In particular, core pattern appeared to be less frequent in the patients who were alive without any problems than in the other patients (33 vs. 83%; $p = 0.08$).

Discussion

In this study, we sought to evaluate the usefulness of HBP in MRI for diagnosing HEH. The result of our study showed that ring-like arterial enhancement and core pattern were frequent in HEH patients, which may aid diagnosis in difficult cases. Radiologic features described in previous reports suggest that HEH often presents as a single nodular and solitary lesion, which may progress to multiple coalescent tumors involving the entire liver. According to a previous report of MRI findings of HEH, a multi-layered appearance with prominent hyperintense rim on T1-weighted and hypointense rim on T2-weighted images corresponds to thrombosed vascular channels at the tumor periphery [15]. In the present study, 20 nodules showed peripheral high signal intensity on T1-weighted images and 16 showed peripheral low signal intensity on T2-weighted images (43% and 34%, respectively). In comparison, core

Table 4. MRI, pathologic features, and clinical courses of individual cases

Hospital	Patient	Age	Sex	Number of lesions	MRI features				Pathologic features (surgical specimen)	Treatment and prognosis
					Core Pattern	Coalescent	Capsular retraction	Entrapment-like pattern		
A	1	52	F	>5	Dominant	Present	Present	Minor		Progression of pulmonary metastases PET-CT at time of diagnosis revealed multiple pulmonary metastases, which showed progression on the second year of follow-up (last follow-up) Patient did not receive any treatment.
	2	42	M	>5	Minor	Present	Present	Minor		Alive, without treatment Minimal change observed with regular follow-up for over 4 years
	3	44	F	>5	Mixed	Absent	Present	Mixed	Central necrosis	Expired, after transplantation Liver transplantation was performed shortly after diagnosis. Liver transplantation was performed again after 18 months due to biliary cirrhosis. Afterward, patient expired due to transplant-related complications (biliary stenosis and cast formation)
	4	37	M	3	Dominant	Absent	Present	Minor		Loss to follow-up
	5	53	F	1	Minor	Absent	Absent	Dominant	Abundant collagen fiber	Alive, after partial hepatectomy Surgical resection was performed 8 years after diagnosis
	6	71	M	>5	Dominant	Present	Present	Minor	High cellularity, No necrosis	Expired, after transplantation Initial work-up did not show metastasis. Patient received liver transplantation from a living donor 9 months after diagnosis. One year after surgery, metastasis was found on imaging
B	7	59	M	>5	Mixed	Present	Present	Minor	Central necrosis	Alive, after partial hepatectomy
	8	40	F	1	Minor	Absent	Present	Minor	Relatively abundant fibrosis	Alive, after partial hepatectomy
	9	81	F	>5	Dominant	Present	Present	Minor		Loss to follow-up
	10	53	F	2	Minor	Absent	Present	Mixed	Abundant collagen fiber	Alive, after partial hepatectomy
	11	42	M	>5	Mixed	Present	Absent	Minor	Central necrosis	Alive, after partial hepatectomy
	12	33	M	>5	Minor	Present	Absent	Dominant		Loss to follow-up

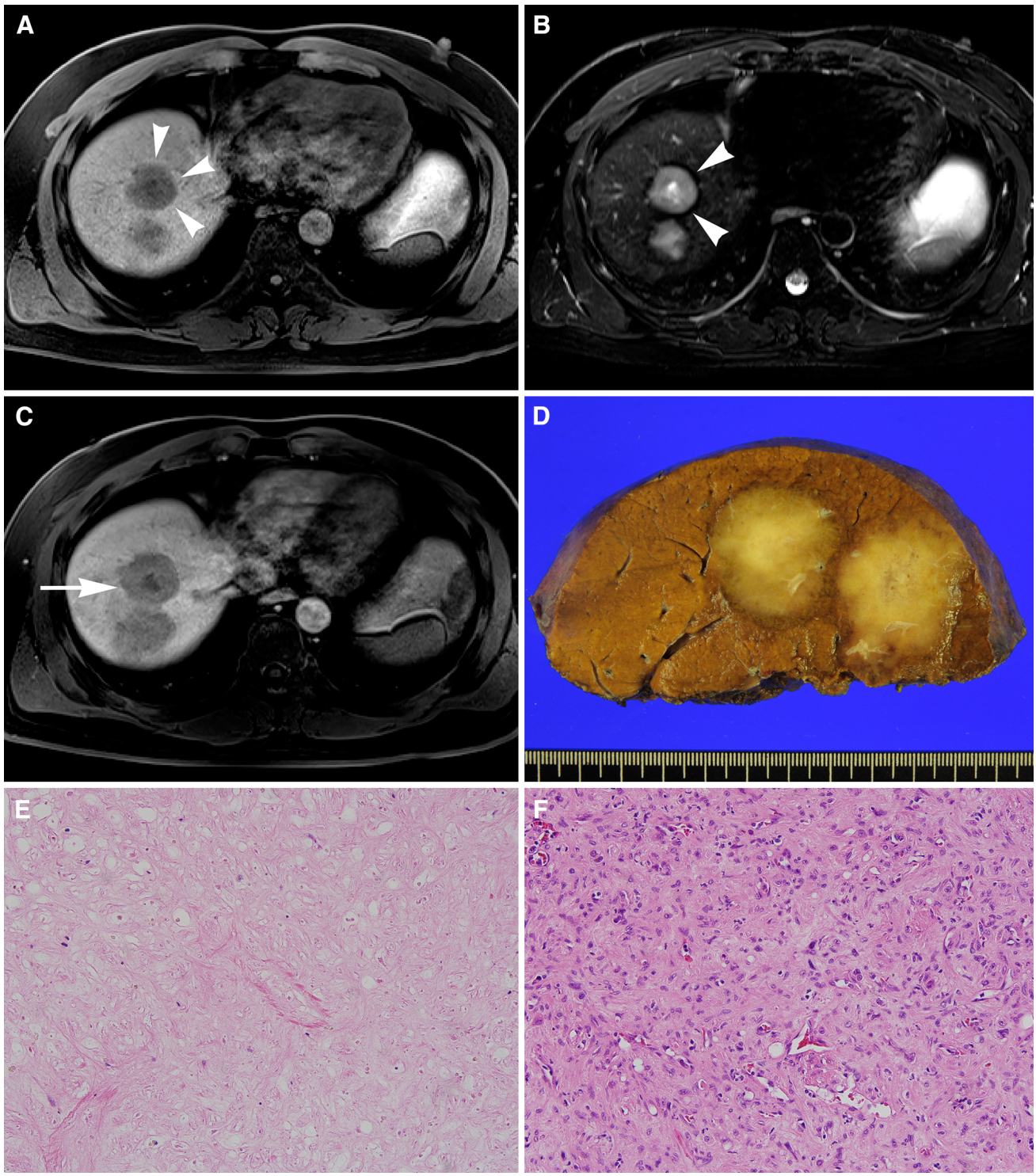

Fig. 4. A 42-year-old male patient who underwent surgical resection. T1- (**A**) and T2-weighted images **B** show a round mass with a subtle hyperintense rim (*arrowheads*) and a definite hypointense rim (*arrowheads*) around the tumor. Hepatobiliary phase after administration of Gd-EOB-DTPA **C** shows a central hypointense core (core pattern; *arrow*). On the gross specimen (**D**), round and lobulated tumors with a central whitish core are noted. In the center of the tumor (**E**), mainly pale-staining necrotic tissues are seen. In contrast, there are many spindle and epithelioid tumor cells infiltrating hepatic sinusoidal spaces in the periphery of the tumor (**F**) (H&E, X100; E&F).

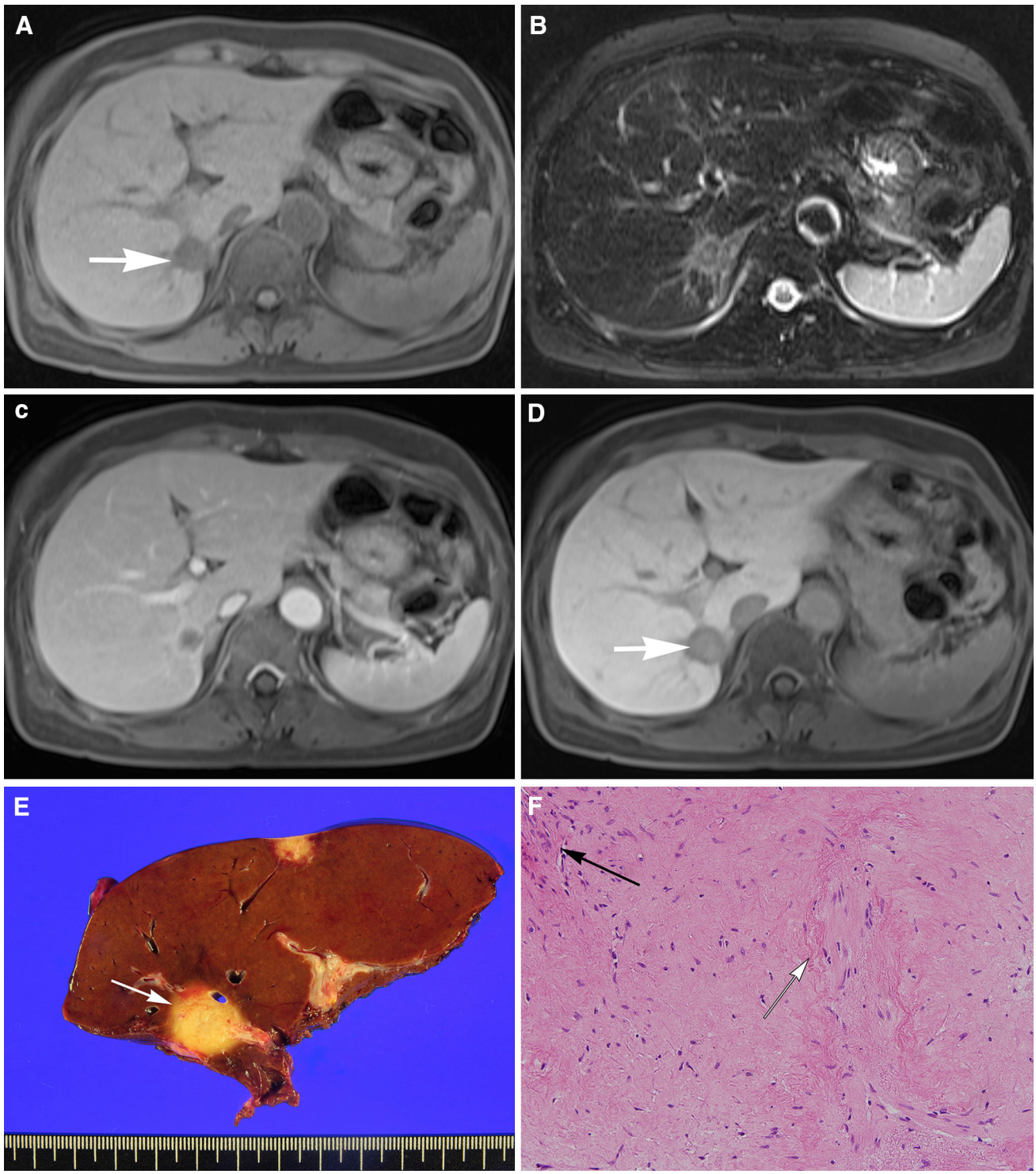

Fig. 5. A 53-year-old female patient who underwent right hemihepatectomy. A round tumor (*arrow*) is visible in segment VII with capsular retraction (**A**), and has peripheral hyperintensity and central hypointensity on T2-weighted images (**B**). After administration of Gd-EOB-DTPA, portal venous phase image shows that the tumor is peripherally enhanced (**C**), and hepatobiliary phase image shows central hyperintensity (*arrow*), the so-called entrapment-like pattern (**D**). The gross specimen shows a homogeneously yellowish solid tumor (*arrow*) (**E**). Representative microscopic picture shows relatively sparse epithelioid tumor cells (*arrow*) embedded in abundant fibrotic and sclerotic stroma (*open arrow*) (H&E, X100; **F**).

pattern was more frequently observed (n = 24; 51%) as well as ring-like enhancement on arterial phase(n = 35; 74%). In the present study, the core pattern of HEH was different from general features of hepatic metastasis from extrahepatic malignancies. Hepatic metastasis generally contains central necrosis with an irregular border and peripherally enhancing viable portions, whereas the core pattern in our cases was clearly a circular core with thick peripheral area of the tumor that was less enhanced than hepatic parenchyma (Fig. 4) [16].

Interestingly, on quantitative analysis, the lesion periphery and center showed different kinetics between the core and non-core lesions. In the non-core group, the SI_{st} of the center was lower than, but approximated, the periphery up to the transitional phase. Although this relationship was reversed on HBP, the center and periphery graphs followed a similar course. In contrast, in the core group, the SI_{st} of the center remained low up to the transitional phase and increased markedly only after that phase, resulting in a substantial difference from the periphery. The fact that the center and periphery show different kinetics, probably reflecting differences in the mode of contrast distribution, suggests different histologic composition between the two regions. More specifically, considering the slow but continuous increase in central signal intensity, we may speculate that the central portion of the lesion is hypocellular and poorly vascularized compared with the periphery, with more myxoid stroma and necrotic tissue instead. Another point of interest is that the center of the entrapment-like lesions, which showed hyperintensity on HBP, consisted of abundant collagen fibers suggestive of fibrotic stroma on pathologic examination (Fig. 5). This seems to be similar to the EOB cloud in intrahepatic cholangiocarcinoma, and central desmoplasia is a frequent finding in HEH. Therefore, both the core and entrapment-like pattern could be aptly explained by the zonal difference seen on pathological examination. This zonal difference has been used to explain other radiological features in previous studies.

Another intriguing finding was that the overall SI_{st} of the core group showed lower values than that of the non-core group throughout all dynamic phases, except for tumor periphery on HBP. This implies that the overall tumor vascularity of core-type tumors may be lower than that of the non-core type.

To date, the prognostic factors of HEH remain unclear, with some authors reporting the presence of symptoms, older age, or elevated serum carbohydrate antigen 19-9 as possible negative prognostic factors [2]. In the present study, the non-core pattern of HEH indicated a better prognosis, adding another potential prognostic factor. Although elaborate explanation of this phenomenon is difficult, given the pathologic features of the core pattern tumors, we cautiously speculate that hypovascularity and central necrosis are negative prognostic factors for HEH. To our knowledge, this has not been suggested before and should be evaluated in future studies.

Since the introduction of hepatobiliary-specific contrast agents, their usefulness in differentiating various focal liver lesions has been extensively examined. To the best of our knowledge, however, there are only two reports on the features of HEH on HBP. A study by Paolantonio et al., which concisely examined the features of HEH on MRI including findings on the HBP, reported that two types of enhancement were noted on HBP [13]. The more common finding was homogeneously low signal intensity, followed by an 'entrapment-like' pattern, which consisted of an enhancing center with a low-signal-intensity rim. The authors likened the 'entrapment-like' pattern to a target appearance, which is similar to the findings of our study albeit with inverted signal intensity. In our study, two patients (17%) showed dominance of the entrapment-like pattern, and two other patients had a mixed pattern of entrapment and non-entrapment.

The other study focused on MRI findings on the HBP, but involved two types of contrast agent with Gd-BOPTA used in the majority of cases (5 of total 6 cases) [14]. Approximately half of the lesions in their study showed hyper- or iso-signal intensity on HBP, but the enhancement pattern might be different across contrast agents, as noted by the authors as a limitation of their study. Therefore, our report is the first to focus on HBP using only Gd-EOB-DTPA, which is a hepatobiliary-specific contrast agent known for its favorable enhancement profile for hepatobiliary imaging, in a relatively large number of cases [17].

Nevertheless, limitations of our study include a small patient number for statistical analysis, retrospective design, sampling error, and inherent relativity of conventional MR signal intensity. Sampling errors may have occurred in several stages. We selected up to five lesions per patient, but many of these patients had more than five lesions. Also, although we averaged the signal intensity after three measurements, a more elaborate segmentation process would have yielded more accurate results. MR signal intensity is inherently relative, which makes it difficult to analyze quantitatively. We attempted to standardize the signal intensity using signal intensity measured from the back muscles, but using a true absolute unit of measurement would yield results that are more reliable. Regarding qualitative analysis, consensus process may have mainly reflected the staff radiologist's interpretation, due to the gap in experience.

In conclusion, the core pattern using Gd-EOB-DTPA could be one of the characteristic MR features of HEH in addition to several previously reported features, and has a pathological basis. Recognition of the core pattern might help in the accurate diagnosis of HEH.

Compliance with ethical standards

Funding No funding was received for this study.

Conflict of Interest The authors declare that they have no conflict of interest.

Ethical approval All procedures performed in studies involving human participants were in accordance with the ethical standards of the institutional and/or national research committee and with the 1964 Helsinki declaration and its later amendments or comparable ethical standards.

Informed consent Need of informed consent was waived since this study was performed retrospectively.

References

1. Mehrabi A, Kashfi A, Fonouni H, et al. (2006) Primary malignant hepatic epithelioid hemangioendothelioma: a comprehensive review of the literature with emphasis on the surgical therapy. Cancer 107:2108–2121. doi:10.1002/cncr.22225
2. Choi KH, Moon WS (2013) Epithelioid hemangioendothelioma of the liver. Clin Mol Hepatol 19:315–319. doi:10.3350/cmh.2013.19.3.315
3. Lyburn ID, Torreggiani WC, Harris AC, et al. (2003) Hepatic epithelioid hemangioendothelioma: sonographic, CT, and MR imaging appearances. AJR Am J Roentgenol 180:1359–1364. doi:10.2214/ajr.180.5.1801359
4. Bruegel M, Muenzel D, Waldt S, Specht K, Rummeny EJ (2011) Hepatic epithelioid hemangioendothelioma: findings at CT and MRI including preliminary observations at diffusion-weighted echo-planar imaging. Abdom Imaging 36:415–424. doi:10.1007/s00261-010-9641-5
5. Makhlouf HR, Ishak KG, Goodman ZD (1999) Epithelioid hemangioendothelioma of the liver: a clinicopathologic study of 137 cases. Cancer 85:562–582
6. Lauffer JM, Zimmermann A, Krahenbuhl L, Triller J, Baer HU (1996) Epithelioid hemangioendothelioma of the liver. A rare hepatic tumor. Cancer 78:2318–2327
7. Amin S, Chung H, Jha R (2011) Hepatic epithelioid hemangioendothelioma: MR imaging findings. Abdom Imaging 36:407–414. doi:10.1007/s00261-010-9662-0
8. Jurczyk M, Zhu B, Laskin W, Lin X (2014) Pitfalls in the diagnosis of hepatic epithelioid hemangioendothelioma by FNA and needle core biopsy. Diagn Cytopathol 42:516–520. doi:10.1002/dc.22943
9. Leonardou P, Semelka RC, Mastropasqua M, Kanematsu M, Woosley JT (2002) Epithelioid hemangioendothelioma of the liver. MR imaging findings. Magn Reson Imaging 20:631–633
10. Dong A, Dong H, Wang Y, et al. (2013) MRI and FDG PET/CT findings of hepatic epithelioid hemangioendothelioma. Clin Nucl Med 38:e66–73. doi:10.1097/RLU.0b013e318266ceca
11. Seale MK, Catalano OA, Saini S, Hahn PF, Sahani DV (2009) Hepatobiliary-specific MR contrast agents: role in imaging the liver and biliary tree. Radiographics 29:1725–1748. doi:10.1148/rg.296095515
12. Song KD, Jeong WK (2015) Benign nodules mimicking hepatocellular carcinoma on gadoxetic acid-enhanced liver MRI. Clin Mol Hepatol 21:187–191. doi:10.3350/cmh.2015.21.2.187
13. Paolantonio P, Laghi A, Vanzulli A, et al. (2014) MRI of hepatic epithelioid hemangioendothelioma (HEH). J Magn Reson Imaging 40:552–558. doi:10.1002/jmri.24391
14. Cieszanowski A, Pacho R, Anysz-Grodzicka A, et al. (2013) Epithelioid hemangioendothelioma of the liver: the role of hepatobiliary phase imaging for the preoperative diagnosis and qualification of patients for liver transplantation – preliminary experience. Ann Transplant 18:424–433. doi:10.12659/AOT.883997
15. Economopoulos N, Kelekis NL, Argentos S, et al. (2008) Bright-dark ring sign in MR imaging of hepatic epithelioid hemangioendothelioma. J Magn Reson Imaging 27:908–912. doi:10.1002/jmri.21052
16. Goodwin MD, Dobson JE, Sirlin CB, Lim BG, Stella DL (2011) Diagnostic challenges and pitfalls in MR imaging with hepatocyte-specific contrast agents. Radiographics 31:1547–1568. doi:10.1148/rg.316115528
17. Jeong WK, Kim YK, Song KD, Choi D, Lim HK (2013) The MR imaging diagnosis of liver diseases using gadoxetic acid: emphasis on hepatobiliary phase. Clin Mol Hepatol 19:360–366. doi:10.3350/cmh.2013.19.4.360